

Exploration of Supramolecular Synthons and Molecular Recognition Starting from Macroscopic Measurements of Crystal Dimensions

Alessia Bacchi,* Giulia Cantoni, Davide Cremona, Paolo Pelagatti, and Franco Ugozzoli

The complete control over the fabrication of crystalline materials is focused nowadays on a bottom-up philosophy that ideally starts with the design and synthesis of good building blocks for assembling a functional material,^[1] proceeds with the prediction of how the molecular units will self-assemble in the crystal,^[2] deals with the nucleation of the correct crystal form,^[3] continues with the growth of final materials with a predetermined shape,^[4] and ultimately relates macroscopic properties to the geometry and strength of the intermolecular interactions.^[5] Here we explore the reverse approach: we analyze and measure the macroscopic morphologies of crystals of a single organometallic compound (**1**) obtained from different solvents in order to identify and rank the intermolecular forces responsible for molecular self-recognition, and then we test and quantify how the functional groups of **1** interact with different solvents.

Compound **1**^[6] was crystallized from six different purified solvents (CH_2Cl_2 , CH_3NO_2 , CH_3OH , $n\text{-CH}_3\text{CH}_2\text{CH}_2\text{OH}$, CH_3CN , $\text{CH}_2\text{Cl}_2/\text{H}_2\text{O}$), giving the same monoclinic nonsolvate crystals, whose nicely faceted morphology is defined by the four forms $\{001\}$, $\{010\}$, $\{\bar{1}01\}$, and $\{\bar{1}\bar{1}1\}$ (a form is the collection of all faces equivalent by symmetry; Figure 1). Compound **1** always crystallizes in platelets, with a prominent basal pair of faces form $\{001\}$, and a lateral envelope made up of the other three forms, which develop to different extents depending upon the solvent used. This suggests that molecular recognition at the solid–solution interface during crystal growth is very effective for the chemical groups exposed at the surfaces constituting the lateral forms,^[7] and points to kinetic control of the final shape. A reliable description of molecular recognition processes in organometallic compounds is particularly difficult, as these compounds with so many electrons are too demanding for state-of-the-art protocols of crystal structure prediction. In fact, **1** contains many functional groups that can function as supramolecular synthons.^[1] While it is well known that the presence of a metal center alters the electron distribution in the ligands and

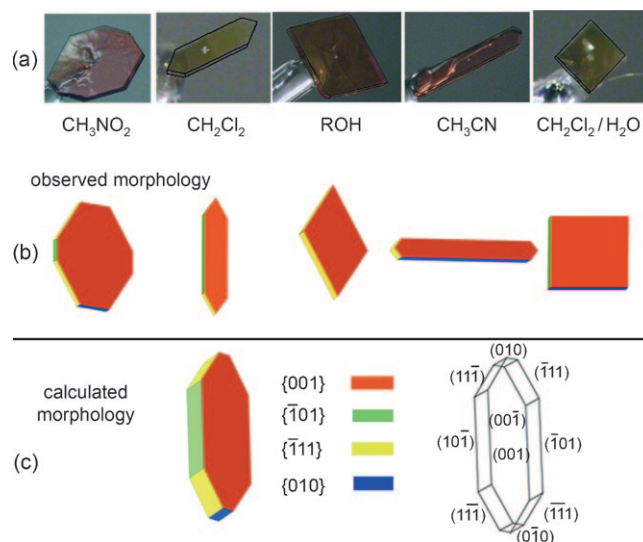


Figure 1. Morphologies of **1** a) depending on the solvent (ROH: CH_3OH and $n\text{-CH}_3\text{CH}_2\text{CH}_2\text{OH}$ give the same morphology) and b) averaged on different crystals for each crystallization experiment; c) ideal morphology, calculated as described in the text.

influences heavily the energy of intermolecular interactions,^[8] most of the recent studies on the crystal packing of organometallic compounds are based on purely geometrical considerations, and few reports deal with the energy of the supramolecular interactions.^[9] We have investigated the supramolecular synthons that stabilize the crystal packing of **1** without relying on considerations of intermolecular distances, which in some cases have been questioned.^[10]

According to Hartman and Perdok,^[11] the $\{hkl\}$ forms shown in Figure 1 should consist of the slowest growing flat faces. These are stable slices of molecules assembled by at least two nonparallel arrays $[uvw]$ of strong supramolecular interactions (periodic bond chains) running along the layer (Figure 2a). We assume that these arrays are built by the most important supramolecular synthons that connect pairs of molecules aligned along $[uvw]$ in the crystal packing of **1**. By analyzing the stereographic projection (see the Supporting Information)^[12] we can deconvolute four main directions $[uvw]$ of molecular arrays that build up the observed crystal faces (hkl) and consequently define the principal supramolecular synthons (SYN) for **1** (Figure 3). Remarkably, while molecular pairs running along $[010]$ could have easily been labeled as hydrogen bonds [SYN1 $\text{OH}\cdots\text{Cl}$ ($1/2-x, y-1/2, 1/2-z$) = 3.170(1) Å, 161(2)°; SYN2 $\text{CH}\cdots\text{Cl}$ ($-1/2-x, y-1/2, 1/2-z$) = 3.534(2) Å, 124(1)°] by a routine analysis of the packing (see the Supporting Information), intermolecular contacts SYN3 along $[100]$ (minimum $\text{C}\cdots\text{C}$ = 3.567 Å) and

[*] Prof. A. Bacchi, Dr. G. Cantoni, D. Cremona, Prof. P. Pelagatti, Prof. F. Ugozzoli
Dipartimento di Chimiche G.I.A.F.
Parco Area delle Scienze 17/A, 43124 Parma (Italy)
Fax: (+39) 0521-905-557
E-mail: alessia.bacchi@unipr.it

Supporting information for this article (including details of the experimental procedures, X-ray analysis, crystal measurements, and DFT calculations) is available on the WWW under <http://dx.doi.org/10.1002/anie.201006561>.

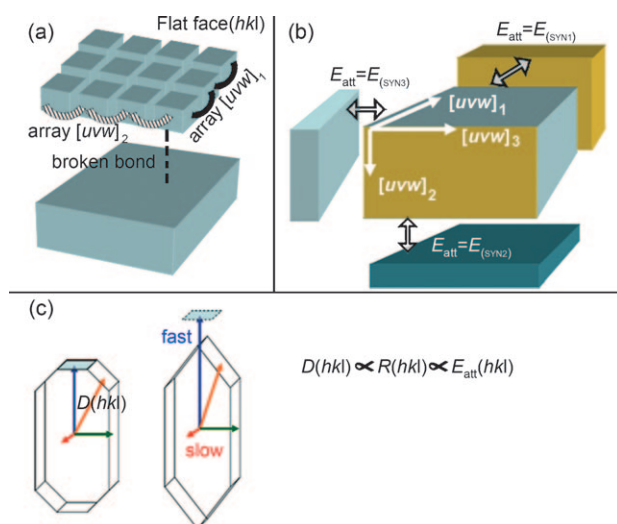


Figure 2. a) Flat faces are built by nonparallel arrays of strong interactions along $[uvw]$; b) the attachment energy E_{att} can be related to broken interactions sticking out of the face; c) Wulff plot relates E_{att} to morphology (left); the fastest growing faces disappear from the final morphology (right).

SYN4 $[101]$ (minimum $C \cdots C = 3.588 \text{ \AA}$) are slightly longer than the van der Waals limits, and would have been neglected. The relevance of these synthons to the packing was quantified by calculating the binding energy of the four molecular pairs that generate the molecular arrays by symmetry replication along $[uvw]$. Single-point calculations (see the Supporting Information) were carried out using DFT methods which include a dispersion term and BSSE corrections (Figure 3), confirming the preponderance of contacts commonly labeled as hydrogen bonds in the packing stabilization, but most

importantly highlighting how also weaker interactions control the supramolecular assembly during crystal growth.

The information gained on the active supramolecular synthons can be exploited to calculate the ideal morphology that **1** would present without the influence of the solvent, and to estimate the solvation energy for each face. It is commonly assumed^[13] that the growth rate $R(hkl)$ of a face is linearly proportional to its attachment energy $E_{att}(hkl)$, defined as the energy per molecule required to split a slice of the face from the crystal bulk by breaking the intermolecular bonds sticking out perpendicularly from the face (Figure 2b). Here we derive the attachment energy of a face as the sum of the energies of the supramolecular synthons crossing the face divided by the number of molecules lying on the face (Table 1 and the Supporting Information). The growth morphology of **1** is simulated by building a Wulff plot where the distance of each face (hkl) from the crystal center $D(hkl)$, representing the growth rate $R(hkl)$, is set equal to $E_{att}(hkl)$ (Figure 2c). It compares very well with the appearance of the crystals obtained from CH_3NO_2 and CH_2Cl_2 ; this shows that supramolecular synthons deduced by analyzing faces indexes are effectively controlling crystal growth (Figure 4). On the other

Table 1: Estimated attachment energies E_{att} and solvation energies E_{solv} (kJ mol^{-1}) of the different faces of **1**. In all cases the fastest growing face was taken as the reference ($E_{solv} = 0$). Faces not observed (italics) are assumed to grow at the same rate as the ideal ones ($E_{solv} = 0$).

Face	E_{att}	E_{solv}				
		CH_3NO_2	CH_2Cl_2	ROH	CH_3CN	$\text{CH}_2\text{Cl}_2/\text{H}_2\text{O}$
(001)	-16.42	-13.06	-11.29	-12.57	-13.83	-12.68
(<i>1</i> 01)	-34.83	0	-15.13	0	0	0
(<i>1</i> 11)	-58.39	-25.17	-6.72	-29.67	-30.58	0
(010)	-90.67	-52.03	0	0	-85.89	-55.36

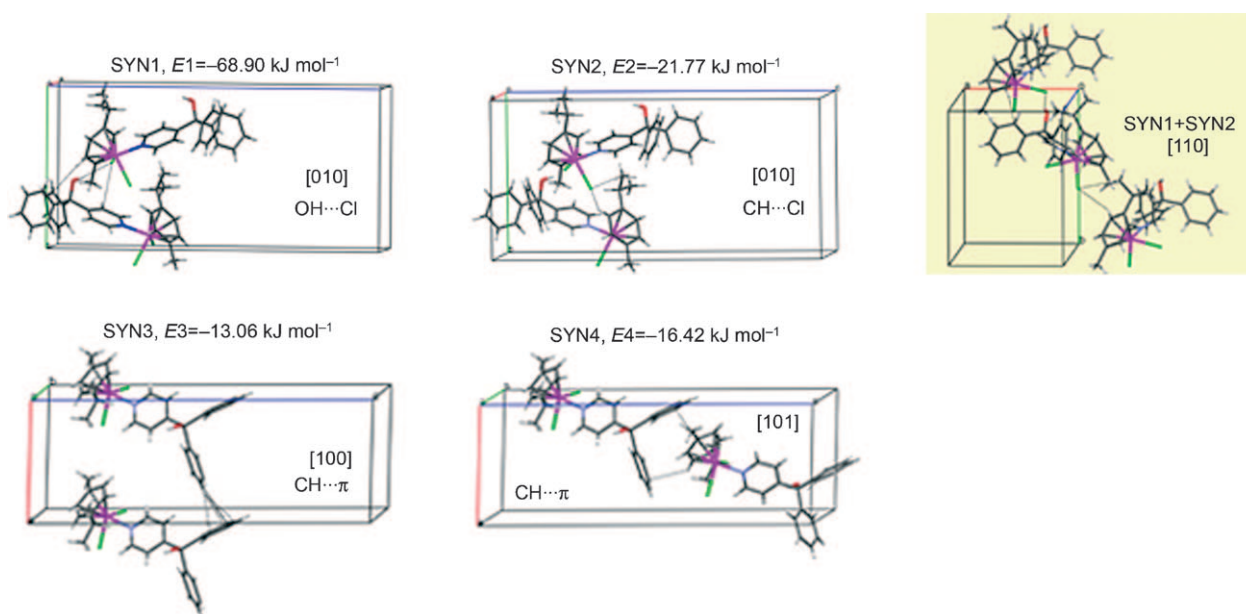


Figure 3. Molecular pairs that generate the four main supramolecular arrays in the crystal packing of **1**. Color legend: C gray, H white, Cl green, N blue, O red, Ru magenta.

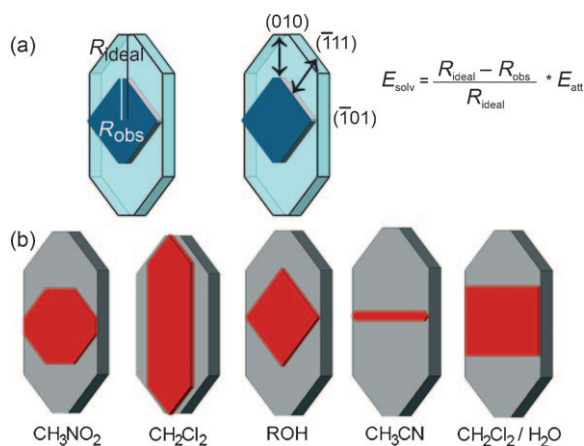


Figure 4. a) The solvation energy $E_{\text{solv}}(hkl)$ of a surface is estimated by comparing the ideal growth rate calculated on the basis of the four supramolecular synthons (R_{ideal}) with the observed one estimated as the distance of a face from the crystal center (R_{obs}). b) Effect of the solvents on the observed morphology (red) compared with the ideal one (gray).

hand, the solvent-dependent modulation of crystal morphology exhibited by crystals obtained from ROH, CH₃CN, and CH₂Cl₂/H₂O indicates that solvents interact with the growing faces and slow down selectively the growth rate of the four $\{hkl\}$ forms by specific molecular recognition events that block growth sites.^[8a,b] A reduced growth rate $R_{\text{obs}}(hkl)$ implies that the attachment energy on a face, $E'_{\text{att}}(hkl)$, is reduced by the solvation energy E_{solv} , defined as the energy necessary to remove a layer of solvent from the surface before the solute is deposited: $R_{\text{obs}}(hkl) \propto E'_{\text{att}}(hkl) = E_{\text{att}}(hkl) - E_{\text{solv}}(hkl)$.^[14] By considering the relative reduction of dimensions of the crystals compared to the ideal model (Figure 4) we computed E_{solv} for the different faces (Table 1), whose surface structure is shown in Figure 5. These are lower

limits for E_{solv} assuming that at least one face, the fastest growing, taken as reference, is not affected by the solvent ($E_{\text{solv}} = 0$). For faces not observed experimentally, upper limits of $E_{\text{solv}}(010)$ in ROH and $E_{\text{solv}}(\bar{1}11)$ in CH₂Cl₂/H₂O may also be estimated by taking the minimum value of $R(hkl)$ required for the face to disappear from the experimental shape (see Table S-I-8 in the Supporting Information). Since the standard deviation for the crystal dimensions does not exceed 15% (see the Supporting Information), the same fraction of the highest E_{solv} (13 kJ mol⁻¹) is taken as the maximum uncertainty on energy values. Hence CH₂Cl₂ does not affect significantly the growth of any of the visible faces, while all the other solvents interact differently with the groups exposed at the surfaces. The $\{001\}$ and $\{\bar{1}01\}$ surfaces are covered by phenyl groups, hence they are the most robust and less sensitive to the solvent ($E_{\text{solv}} \leq 15$ kJ mol⁻¹), since solvent–phenyl interactions cannot compete with solute–solute interactions. The surfaces of $\{\bar{1}11\}$ are rich in Cl ligands, which are good hydrogen-bond acceptors;^[8] hence it is moderately affected (25–31 kJ mol⁻¹) by the weak hydrogen-bond donors ROH, CH₃NO₂, and CH₃CN. The $\{010\}$ surfaces are rich in exposed OH and Cl groups; hence they are the most affected by most of the solvents (observed values 40–86 kJ mol⁻¹), with a generally high E_{solv} . Apart from CH₂Cl₂ all the solvents examined here are very good hydrogen-bond acceptors and moderate to good donors, so they can partially block the OH and Cl attachment sites of $\{010\}$, and the estimated E_{solv} values are compatible with such a mechanism. Surprisingly, CH₃CN presents the highest E_{solv} for $\{010\}$ even if it is poorer hydrogen-bond acceptor than H₂O or CH₃NO₂.^[15] In fact the $\{010\}$ surfaces expose arrays of OH groups regularly spaced by 8.7 Å that mimic the crystal structure of CH₃CN, in which CH \cdots N hydrogen bonds are spaced by 8.4 Å (Cambridge Structural Database: QQQCIV01). Moreover, 12 structures in the CSD where a CH₃CN molecule bridges two OH groups between 7.5 and 8.7 Å apart. Thus a multipoint recognition of CH₃CN by the OH groups on the $\{010\}$ surfaces could enhance the solvation effect.

Our analysis relies on many assumptions and simplifications on the actual growth mechanism at the molecular level. We assumed non-equilibrium growth morphologies, delimited by flat faces with similar growth rates in response to supersaturation, no influence of nuclei initial shape and of antisolvent, and neglected impurities and defects like screw dislocations. Some of these issues were addressed by experimental design (see the Supporting Information). Later developments of the HP-PBC model consider a roughening process for flat faces, triggered by a

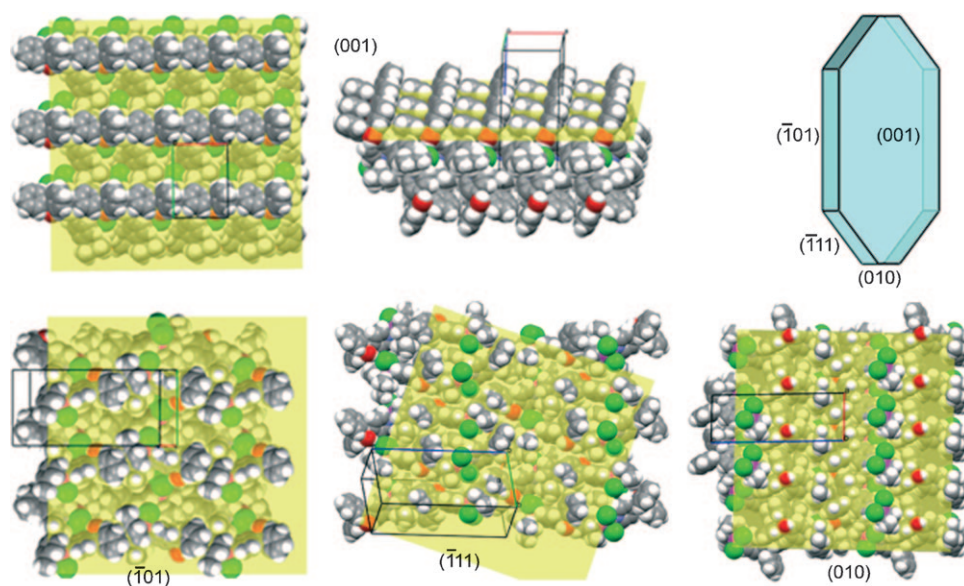


Figure 5. Surfaces structures of the observed faces. Color legend: C gray, H white, Cl green, N blue, O red, Ru magenta.

critical temperature T_R , above which they develop steps and kinks and grow fast into globular ill-shaped crystals by two-dimensional nucleation.^[16] Here we assume to operate below T_R , since we obtain nice and reproducible faceted crystals. We believe that the method described here, although very simple and approximate, can encourage researchers to use all the experimental data, including the simple macroscopic observations that are usually neglected observations,^[17] to reinforce the classical interpretation of molecular interactions that often is carried out only on the basis of geometrical analysis. This approach would be most important for organometallic compounds, where the modeling of supramolecular interactions is presently hindered by computational limitations, as well as for comparison between experimental and calculated solvation energies.

Received: October 19, 2011

Published online: March 2, 2011

Keywords: crystal growth · crystallography · density functional calculations · ruthenium · shape control

- [1] a) *Frontiers in Crystal Engineering* (Eds: E. R. T. Tiekink, J. J. Vittal), Wiley-VCH, Chichester, UK, **2006**; b) G. R. Desiraju, *Crystal Engineering: The Design of Organic Solids*, Elsevier, New York, **1989**; c) G. R. Desiraju, *Angew. Chem.* **2007**, *119*, 8492–8508; *Angew. Chem. Int. Ed.* **2007**, *46*, 8342–8356.
- [2] a) J. D. Dunitz, A. Gavezzotti, *Chem. Soc. Rev.* **2009**, *38*, 2622–2633; b) S. L. Price, *Phys. Chem. Chem. Phys.* **2008**, *10*, 1996–2009.
- [3] a) R. J. Davey, K. Allen, N. Blagden, W. I. Cross, H. F. Lieberman, M. J. Quayle, S. Righini, L. Seton, G. J. T. Tiddy, *Cryst. EngComm* **2002**, *4*, 257–264; b) I. Weissbuch, V. Y. Torbeev, L. Leiserowitz, M. Lahav, *Angew. Chem.* **2005**, *117*, 3290–3293; *Angew. Chem. Int. Ed.* **2005**, *44*, 3226–3229; c) C. S. Towler, R. J. Davey, R. W. Lancaster, C. J. Price, *J. Am. Chem. Soc.* **2004**, *126*, 13347–13353; d) I. Weissbuch, M. Lahav, L. Leiserowitz, *Cryst. Growth Des.* **2003**, *3*, 125–150.
- [4] a) J. M. García-Ruiz, E. Melero-García, S. T. Hyde, *Science* **2009**, *323*, 362–365; b) H. Cölfen, S. Mann, *Angew. Chem.* **2003**, *115*, 2452–2468; *Angew. Chem. Int. Ed.* **2003**, *42*, 2350–2365; c) M. A. Lovette, A. R. Browning, D. W. Griffin, J. P. Sizemore, R. C. Snyder, M. F. Doherty, *Ind. Eng. Chem. Res.* **2008**, *47*, 9812–9833; d) L. Addadi, D. Joester, F. Nudelman, S. Weiner, *Chem. Eur. J.* **2006**, *12*, 980–987.
- [5] a) C. M. Reddy, K. A. Padmanabhan, G. R. Desiraju, *Cryst. Growth Des.* **2006**, *6*, 2720–2731; b) D. Das, T. Jacobs, L. J. Barbour, *Nat. Mater.* **2010**, *9*, 36–39.
- [6] Crystal data: monoclinic, space group $P2_1/c$, $a = 8.7260(3)$ Å, $b = 11.7532(4)$ Å, $c = 24.2247(8)$ Å, $\beta = 92.158(1)^\circ$, $V = 2482.7(1)$ Å³; $Z = 4$.
- [7] a) I. Weissbuch, L. Addadi, M. Lahav, L. Leiserowitz, *Science* **1991**, *253*, 637–645; b) M. Lahav, L. Leiserowitz, *Cryst. Growth Des.* **2006**, *6*, 619–624; c) D. Winn, M. F. Doherty, *AIChE J.* **2000**, *46*, 1348–1367.
- [8] a) L. Brammer, *Chem. Soc. Rev.* **2004**, *33*, 476–489; b) C. Janiak, *J. Chem. Soc. Dalton Trans.* **2000**, 3885–3896; c) L. Brammer, *Dalton Trans.* **2003**, 3145–3157.
- [9] a) A. Kovacs, Z. Varga, *Coord. Chem. Rev.* **2006**, *250*, 710–727; b) E. Peris, J. C. Lee, J. R. Rambo, O. Eisenstein, R. H. Crabtree, *J. Am. Chem. Soc.* **1995**, *117*, 3485–3491; c) J. Breu, H. Domel, P.-O. Norrby, *Eur. J. Inorg. Chem.* **2000**, 2409–2419.
- [10] a) G. R. Desiraju, *Acc. Chem. Res.* **2002**, *35*, 565–573; b) I. Dance, *New J. Chem.* **2003**, *27*, 22–27.
- [11] a) P. Hartman, W. G. Perdok, *Acta Crystallogr.* **1955**, *8*, 49–52; b) P. Hartman, W. G. Perdok, *Acta Crystallogr.* **1955**, *8*, 521–524; c) P. Hartman, W. G. Perdok, *Acta Crystallogr.* **1955**, *8*, 525–529; d) P. Bennema, H. Meekes, S. X. M. Boerrigter, H. M. Cuppen, M. A. Deij, J. van Eupen, P. Verwer, E. Vlieg, *Cryst. Growth Des.* **2004**, *4*, 905–913.
- [12] G. Pfeifer, R. Boistelle, *J. Cryst. Growth* **2000**, *208*, 615–622.
- [13] P. Hartmann, P. Bennema, *J. Cryst. Growth* **1980**, *49*, 145–156.
- [14] a) J. H. ter Horst, R. M. Geertman, G. M. van Rosmalen, *J. Cryst. Growth* **2001**, *230*, 277–284; b) J. Chen, B. L. Trout, *Cryst Growth Des.* **2010**, *10*, 4379–4388.
- [15] C. A. Hunter, *Angew. Chem.* **2004**, *116*, 5424–5439; *Angew. Chem. Int. Ed.* **2004**, *43*, 5310–5324.
- [16] R. F. P. Grimbergen, H. Meekes, P. Bennema, C. S. Strom, L. J. P. Vogels, *Acta Crystallogr. Sect. A* **1998**, *54*, 491–500.
- [17] One century ago P. von Groth reviewed the morphologies of thousands of compounds with the aim of deriving the crystal structure from the morphology. (P. v. Groth, *Chemische Kristallographie*, Vols. 1–5, Verlag Wilhelm Engelmann, Leipzig, **1906–1919**). This approach was abandoned with the development of X-ray diffraction, and information on morphology was progressively neglected in routine crystal structure analyses.